Journal of Inorganic and General Chemistry
ZAAC
Zeitschrift für anorganische und allgemeine Chemie
www.zaac.wiley-vch.de
RESEARCH ARTICLE
DOI: 10.1002/zaac.202100380

A caveat on the effect of modulators in the synthesis of the aluminum furandicarboxylate metal-organic framework MIL-160

Dominik Moritz Steinert,[a] Alexa Schmitz,[a] Marcus Fetzer,[a] Philipp Seiffert,[a] and Christoph Janiak*[a]

Dedicated to Prof. Dr. Caroline Röhr on the occasion of her 60th birthday.

Modulators are widely used in the synthesis of metal-organic frameworks (MOFs) for improving the porosity and morphology. For aluminum MOFs modulation has been seldom reported and as is shown here for the example of the aluminum furandicarboxylate MOF MIL-160 the positive effects of modulators are small and disadvantageous effects will be more likely. Formic acid as modulator can slightly increase the BET surface area and pore volume of MIL-160 up to a modulator:linker ratio of 1.25 : 1. Acetic acid only shows some increase in both surface area and pore volume at the smallest tested ratio of 0.125 : 1. The stronger acids oxalic acid and hydrochloric acid with the also more aluminum-coordinating anions have no positive porosity effect and decrease surface area and pore volume already at small amounts. At a 1 : 1 modulator:linker ratio for oxalic acid and at 0.75 : 1 for hydrochloric acid no porous MOF is formed anymore from the analysis by powder X-ray diffraction and nitrogen sorption. Further, thermogravimetric analysis and scanning electron microscopy suggests that none of the tested modulators has any noticeable positive effect on the introduction of linker defects or the improvement of crystallinity or crystal size.

Introduction

Metal-organic frameworks (MOFs) are crystalline and porous metal-ligand coordination networks.[1–4] MOFs are designable in their properties[5] in many different dimensions, which leads to a still rising scientific and commercial interest in promising applications, such as useful heat transformation,[6–8] catalysis,[9] gas and liquid separation,[10,11] natural gas[12] and methane storage.[13] For applications like ethanol dehydration,[14] or the isosteric heat of adsorption of water[15] it can be necessary to tailor the characteristics of MOFs with respect to morphology, crystal size, porosity and defects,[16–18] e.g., through the use of modulators in their synthesis.[19,20]

The kinetics of the framework formation can be influenced by modulating ligands which bind to the metal ion or cluster with a weaker binding energy than the linker. Thereby, the modulator competes with the linker and, for example, slows the crystal growth process or can in part remain in the MOF and induces linker defects.[3,17,18,21–24] Often used modulators are hydrochloric acid and organic monocarboxylic acids, such as benzoic acid, formic acid, acetic acid or trifluoroacetic acid. In UiO-type Zr-MOFs the increase of linker defects by monocarboxylic acid modulators is used to enhance the porosity and yield.[25] Gökpinar *et al.* observed an increase in BET surface areas, as well as increasing yields when HCl was used as modulator in UiOs.[26] Lazaro *et al.* for example used a MOF with modulation-increased defects for anti-cancer drug delivery and Liao *et al.* were able to induce desired types of porosity with templating modulators.[27,28]

The modulation effects on the Al-MOF MIL-160, which is considered here, are derived from the kinetic and thermodynamic reaction behavior of solvated Al^{3+} cation and not necessarily by the MOF which is formed. Hence, different modulation effects are to be expected for MOFs with other metal ions, for example, for the Zr^{4+}-MOFs in the UiO series. The kinetic stability, that is inertness/lability of an existing metal-ligand bond towards ligand exchange will be fundamental in the modulation process, especially if both the modulator and linker feature the same (e.g. carboxylate) donor groups. The kinetic stability correlates with the reaction rate (constant) and activation energy for the process.[29] An estimate of the lability of a metal ion towards ligand exchange can be obtained from the well-known *Merbach* series of rate constants for the exchange of aqua ligands in aqua complexes $\{[M(H_2O)_n]^{c+} + H_2O^* – k(H_2O) \rightarrow [M(H_2O)_{n-1}(H_2O^*)]^{c+} + H_2O\}$.[30–32] The most inert main-group metal ion is Al^{3+} with a rate constant for exchange in the $[Al(H_2O)_6]^{3+}$ complex of $k(H_2O) = 1.3\ s^{-1}$. Thereby, Al^{3+} occupies a middle position in the inert-to-labile classification. Among the three-valent metal ions Al^{3+} is more labile than for

[a] *D. M. Steinert, A. Schmitz, M. Fetzer, P. Seiffert, Prof. C. Janiak*
Institut für Anorganische Chemie und Strukturchemie
Heinrich-Heine-Universität Düsseldorf
40204 Düsseldorf, Germany
E-mail: janiak@uni-duesseldorf.de

Supporting information for this article is available on the WWW under https://doi.org/10.1002/zaac.202100380

example Cr^{3+} ($k(H_2O) = 2.4 \cdot 10^{-6}\ s^{-1}$) but less so than Fe^{3+} ($k(H_2O) = 180\ s^{-1}$) and especially Ti^{3+} ($k(H_2O) = 1.8 \cdot 10^{+5}\ s^{-1}$) or the divalent transition-metal cations from Mn^{2+} to Cu^{2+}. The latter have fast rate constants $k(H_2O)$ of over $10^{+6}\ s^{-1}$. Unfortunately, the rate constant for the aqua ligand exchange in Ti^{4+} has not been determined. Qualitatively, Ti^{4+} may be regarded as more labile than Al^{3+} because of its larger size and thereby more open coordination sphere for attacks towards nucleophilic substitution through an associative mechanism. Thermodynamically, the high-valent metal atoms Zr^{4+}, Cr^{3+} and Al^{3+} form stronger metal-carboxylate ligand bonds than divalent metal ions, simply from the Coulomb energy where the product of cation and anion charge enters in the nominator. Hence, Zr^{4+} may give a higher ionic bond strength by its increased charge than Al^{3+}, although this may be augmented by the high charge density of the smaller Al^{3+} (ionic radius 57 pm) over Zr^{4+} (87 pm).[29]

Thus, the action of modulators is difficult to predict. For example, Zhao *et al.* showed for MIL-101(Cr) that the addition of nitric acid improves both the yield and the porosity of the MOF, compared to the use of problematic hydrofluoric acid, while acetic acid enabled the MOF to be synthesized at lower temperatures and still acceptable surface area.[33] Furthermore, it was found that MIL-101(Cr) crystal growth was suppressed when acetic acid was used as a modulator, which led to smaller particle size.[34,35] Large amounts of acetic acid even changed the crystal phase of the MOF, as was demonstrated by Yang *et al.* with the formation of MIL-88B(Cr) instead of MIL-101(Cr).[36] Moll *et al.* found that the use of very high amounts of mercaptoacetic acid in the synthesis of UiO-66 leads to a phase change from face-centered cubic, fcu to hexagonal close-packed, hcp phase with a different framework structure.[20]

The use of modulators does not even always show beneficial results. Bennett *et al.* discussed decreasing structure flexibility of UiO-66 with rising defect amounts, introduced by the use of monocarboxylic acids as modulator.[37] Even lowered nitrogen sorption abilities were reported based on the use of modulator in aluminum fumarate.[38]

Aluminum-based MOFs like MIL-53,[39] Alfum (Basolite A520),[40–42] CAU-10[43] or MIL-160[44] are among the most promising MOFs for applications due to their chemical and hydrothermal stability.[45–49] Aluminum is an abundant and inexpensive light metal with low toxicity.[46,47,50,51] MIL-160 in particular is a hydrophilic, highly hydrothermally stable Al-MOF (see Section S1, Figure S1 for structure description) with promising water sorption characteristics. MIL-160 was noted as the most promising Al-MOF for heat pump applications as it outperforms both Alfum and CAU-10-H in terms of gravimetric water loadings.[44] MIL-160 is also a highly promising material for adsorptive SO_2 separation and flue gas desulfurization, especially under application orientated conditions, and features excellent SO_2/CO_2 selectivities and $SO_2/N_2/CO_2$ breakthrough performance with high onset time, combined with high stability under both humid and dry SO_2 exposure.[52] The synthesis route of MIL-160 is environmentally friendly, since the linker can be produced from renewable biomass *via* oxidation of 5-(hydroxymethyl)furfural (5-HMF) on a very large industrial scale and water is the single solvent.[53,54] Permyakova *et al.* investigated MIL-160 with respect to shaping into granules and heat reallocation underlining the suitability of the material for heat transformation application.[55]

Modulated Al-MOFs have been very rarely reported. Canossa *et al.* described the influence of oxalic acid for the synthesis of crystalline Al-MOFs and observed an increased particle size. from ~5 nm to ~40 nm.[56] Teo *et al.* presented formic acid modulated Alfum for improved water adsorption. Alfum particles elongate and the synthesis time could be reduced with the addition of formic acid.[57]

In this work we report the influence of the four modulators oxalic acid, formic and acetic acid as well as HCl in the synthesis of MIL-160. To the best of our knowledge there exists no systematic study on the influence of different modulators for aluminum MOFs yet.

Results and Discussion

The synthesis of MIL-160 was carried out following the synthesis from Permyakova *et. al.*[55] by combining basic aluminum diacetate and furandicarboxylic acid in a 1:1 molar ratio in the presence of formic acid, acetic acid, oxalic acid, and hydrochloric acid as modulators in water. The molar ratio of modulator:metal/linker ranged from 0.0625:1 to 2:1. Higher modulator to linker ratios were not investigated as it became evident that ratios of ~1:1 already induced significant disadvantageous and undesired phase and porosity changes.

The effect of modulation was assessed and followed by powder X-ray diffractometry (PXRD) (Figure 1) and porosity characterization through N_2 sorption measurements (Figure S2–S5, Supp. Info.). The PXRD pattern for the formic acid and acetic acid modulated MIL-160 show no significant change in crystal phase even at modulator:metal/linker ratios up to 2:1 (Figure 1a,b). With oxalic acid modulation the PXRD pattern exhibits reflexes for both MOF and crystalline linker at a modulator:metal/linker ratio of 1:1 (Figure 1c). At a ratio of 1.5:1 only the crystalline phase of the linker could be identified. With hydrochloric acid modulation, residual linker is already apparent at a modulator:metal/linker ratio of 0.5:1 (Figure 1d) with its PXRD reflexes and at 1.5:1 only linker reflexes remain.

The BET-surface areas increase slightly only with the modulator formic acid and very low amounts of acetic acid in modulator ratio, albeit at a different extent for each modulator (Table 1, Figure 2 and Table S2–S5). The pore volumes tend to first increase and go through a maximum with added formic and acetic acid modulator before decreasing again (Table 1, Figure 3). With oxalic and hydrochloric acid the pore volumes decrease right away.

For formic acid the BET surface area increases up to a modulator-to-linker ratio of 1.25:1 or at the most increases only very slightly from 1105 $m^2 g^{-1}$ to 1210 $m^2 g^{-1}$. Upon further increase of modulator to 2:1 the surface area drops sharply to 442 $m^2 g^{-1}$. For the acetic acid modulated series, the surface area only increased at a ratio of 0.125:1 and then drops to 900–800 $m^2 g^{-1}$. Oxalic acid modulation starts with an immediate

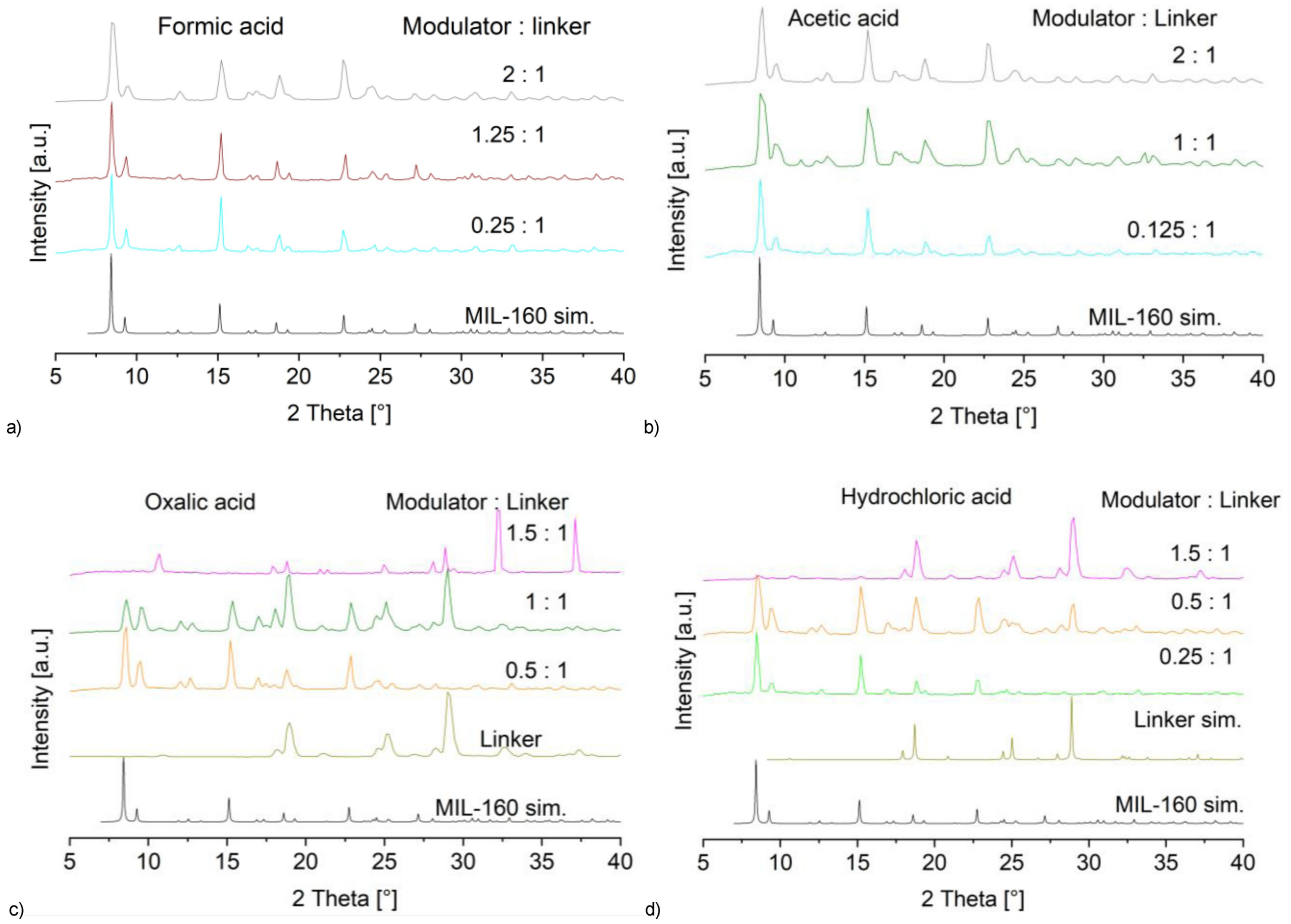

Figure 1. Selected powder X-ray diffraction patterns of MIL-160 synthesized with different modulators and molar modulators:linker ratios as indicated. The simulated diffractogram for MIL-160 is based on the deposited cif file with CCDC no. 1828694, Refcode PIBZOS.[58] The simulated diffractogram for the linker is based on the deposited cif file with CCDC no.11611468, Refcode FURDCA.[59] For diffraction patterns for all used modulator:linker ratios see Fig. S6–S9, SI.

Table 1. BET surface area and pore volume of modulated MIL-160.[a,b]

BET surface [$m^2\ g^{-1}$] (at molar modulator:linker ratio)
1105 (0:1, no modulator)

Formic acid	Acetic acid	Oxalic acid	Hydrochloric acid
1117 (0.125:1)	1197 (0.125:1)	1028 (0.0625:1)	743 (0.25:1)
1210 (1.25:1)	952 (0.75:1)	747 (0.625:1)	531 (0.5:1)
874 (1.75:1)	926 (2:1)	749 (0.875:1)	71 (0.75:1)

Total pore volume [$cm^3\ g^{-1}$] (at molar modulator:linker ratio)
0.43 (0:1, no modulator)

Formic acid	Acetic acid	Oxalic acid	Hydrochloric acid
0.45 (0.125:1)	0.51 (0.125:1)	0.42 (0.0625:1)	0.33 (0.25:1)
0.50 (1.25:1)	0.41 (0.75:1)	0.30 (0.625:1)	0.24 (0.5:1)
0.34 (1.75:1)	0.44 (2:1)	0.28 (0.875:1)	0.06 (0.75:1)

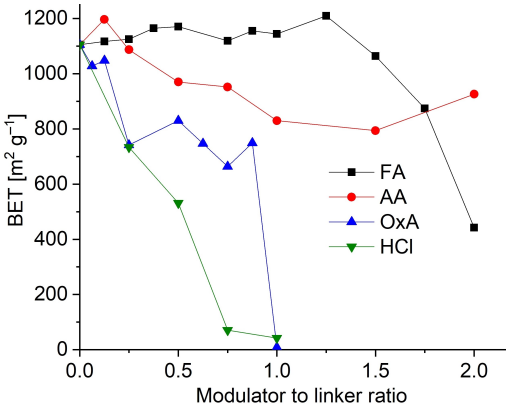

Figure 2. Trends of the BET surface of MIL-160, depending on the modulator to linker ratio of the different modulators. The numbers on the x-axis are always in relation to 1 with respect to the linker amount. The graphs include the values from all tested modulator: linker ratios as given in Table S2–S5, SI.

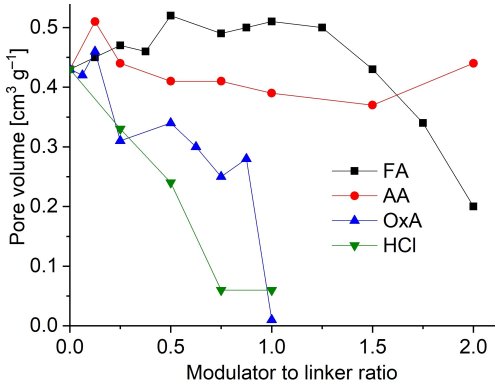

Figure 3. Trends of the total pore volume of MIL-160, depending on the modulator to linker ratio of the different modulators. The numbers on the x-axis are always in relation to 1 with respect to the linker amount. The graphs include the values from all tested modulator:linker ratios as given in Table S2–S5, SI.

decrease at a low ratio of 0.0625:1 already, which continues to about 700 $m^2 g^{-1}$ at a modulator:linker ratio of 0.875:1. At a 1:1 ratio a substantial amount of linker remains unreacted (cf. Figure 1c) and the product mixture is essentially non-porous (9 $m^2 g^{-1}$). The concomitant pore volume of 0.01 $cm^3 g^{-1}$ is due to interparticle voids. The modulator HCl induces also an immediate decrease of the surface area. At a ratio of 0.25:1 the BET surface is already reduced to 743 $m^2 g^{-1}$. With a 0.5:1 ratio the BET surface decreases further to 531 $m^2 g^{-1}$ and for ratios higher than 0.5:1 the BET surface area is little more than the outer surface area of a fine powder.

The total pore volume of formic acid modulated MIL-160 starts from 0.47 $cm^3 g^{-1}$ at 0.125:1 and goes through a maximum of 0.52 $cm^3 g^{-1}$ for 0.5:1 before decreasing with progressing modulator ratio down to 0.43 $cm^3 g^{-1}$ at 1.5:1 and even below with higher ratios. For acetic acid the pore volume varies somewhat in a range from 0.51 to 0.37 $cm^3 g^{-1}$ over the different modulator to linker ratios up to 2:1. For oxalic acid the pore volume decreases from 0.46 at 0.125:1 to 0.28 up to a modulator to linker ratio of 0.875:1. At the 1:1 ratio here, there is no longer a MOF synthesized, just residual linker is present with no BET surface and an only small measured pore volume of 0.01 $cm^3 g^{-1}$. With hydrochloric acid the pore volume decreases from 0.33 $cm^3 g^{-1}$ at a 0.25:1 modulator to linker ratio to 0.24 $cm^3 g^{-1}$ at a 0.5:1 ratio. With higher ratios the pore volume goes down to nearly zero.

Thus, a small amount of modulator can advantageously increase the surface area and pore volume. Formic acid would be the best modulator choice at and up to a modulator:linker ratio of 1.25:1. Acetic acid only shows some increase in both surface area and pore volume at the smallest ratio of 0.125:1, whereas oxalic acid decreases both, the pore volume and the surface area considerably. The mineral acid HCl has no positive porosity effect.

Digestion NMR was used to test for the incorporation of modulator into the MOF. Selected samples which had been synthesized in the presence of high modulator:metal/linker ratio were dissolved und decomposed in 5% NaOD in D_2O. Samples from 2:1 ratios for formic and acetic acid and at a 1:1 ratio for oxalic acid showed no significant remnants of modulator in the samples (Figures S10–13, Supp. Info.).

Thermogravimetric analysis (TGA) was used to test for defects from linkers which were replaced by modulator or H_2O/OH ligands. The method for calculating missing linker-defect sites was adapted from the work of Shearer *et al.*[25,60] for UiO-66 (Section S5, Supp. Info.). Analysis of the TGA curve profiles (Figures S16–23) led to the conclusion that these modulators do not induce significant amounts of missing linker defects in MIL-160 (see Supp. Info. for details). TGA shows in accordance with N_2 sorption and PXRD that at sufficiently high modulator quantities no more MOF is formed. At the above noted modulator-to-linker ratios almost exclusively linker is present in the solid products because the modulator kept the aluminum in solution during the synthesis and thus prevents the formation of the framework. Details are given in the Supp. Info.

The microcrystals of the formic acid and to some extent also the acetic acid modulated series seem to be fused to larger aggregates with increase of modulator (Figure S21, S22, Supp. Info).

The slightly positive effect of small amounts of the organic acid modulators formic acid and acetic acid on the porosity of MIL-160 is probably due to their similarity to the organic acid linker, e.g., in terms of pK_a values (formic acid 3.77, acetic acid 4.75, furandicarboxylic acid 4.38, 5.85[61]). Oxalic and hydrochloric acid are not only stronger acids (pK_a oxalic acid 1.25, hydrochloric acid −7) but also give rise to the formation of oxalato and chlorido complexes with aluminum, e.g., $[Al(ox)_3]^{3-}$ and $[AlCl_4]^-$. The formation of such relatively stable complexes will prevent the MOF formation as was evident in the powder X-ray diffractograms with remaining crystalline linker at a modulator:metal/linker ratio of 1:1 upon oxalic and hydrochloric acid modulation (Figure 1c,d).

Conclusions

The modulators formic acid and acetic acid, show only limited positive effects in the synthesis of the aluminum MOF MIL-160. This adds to the still rather small number of studies on the modulation of aluminum MOFs where also no strong effects could be observed, profoundly different from the significant modulator consequences in zirconium MOFs. For MIL-160 none of the tested modulators has any noticeable positive effect on the introduction of linker defects, the improvement of yield, crystallinity or crystal size. Formic acid up to a modulator:metal/linker ratio of 1.25:1 and acetic acid at the very small ratio of 0.125:1 yielded a small improvement in porosity, that is, BET surface area and pore volume. Above these ratios the BET surface area and eventually the pore volume started to decrease. For the modulators oxalic acid and hydrochloric acid, which interact more strongly with aluminum through complex formation, there was no positive effect on the porosity even for small amounts of modulator. The results do not rule out modulator effects for aluminum MOFs in general but caution

for a careful evaluation before claiming an influence. The effects from the modulator comparison in this study suggest that monocarboxylic acids of similar binding strength to aluminum as the linker should be most promising.

To put these results in context with other studies on the modulation of MOFs, the comparatively small amount of modulator should be noted. The ratio of modulator to linker in this work is below 2, due to side-product formation etc. Whereas, in the modulation of UiO-66 modulator equivalents up to 100 are often used.[20,25] Thus, direct comparison between modulation reactions for Al-based and Zr-based MOFs do not seem appropriate. The difference in modulator amount may be seen as a manifestation of the different lability/inertness of Al^{3+} versus Zr^{4+} (cf. Introduction). It may be concluded that for the more inert Al^{3+} small amounts of modulator can already prevent the MOF formation, leaving unreacted linker as the only identifiable phase.

Experimental Section

Materials and Methods

Basic aluminum diacetate, $Al(OH)(CH_3COO)_2$ was obtained from ChemPur, 2,5-furandicarboxylic acid (97%) from Apollo Scientific, oxalic acid (99.5%) from Acros Organics, formic acid (99%) from VWR Chemicals, acetic acid (99.8%) from Sigma Aldrich and hydrochloric acid (37%) from Fisher Chemicals and used without further purification.

Powder X-ray diffractograms (PXRD), were obtained with a *Bruker D2 Phaser* diffractometer using a flat silicon, low background sample holder and Cu-K_α radiation ($\lambda = 1.54184$ Å) at 30 kV and 0.04° s^{-1} in the $2\theta = 5$–50° range.

Brunauer-Emmett-Teller[62] (BET) surface areas were determined by nitrogen (N_2) (99.999%) sorption at T = 77 K on a *Quantachrome NOVA-4200e or* Autosorb-6 instrument with a relative pressure range of $pp_0^{-1} = 10^{-3}$–1. Each sample (20–50 mg) was degassed under vacuum ($< 10^{-2}$ mbar) at 120 °C for at least 4 h prior to measurement. All BET surface areas were calculated from at least three adsorption data points in the pressure range $0.05 < pp_0 < 0.2$, applying Roquerol plots ($r > 0.998$). The total pore volume was determined at $pp_0^{-1} = 0.95$.

Thermogravimetric analysis (TGA) was measured on a *Netzsch TG 209 F3 Tarsus* under synthetic air atmosphere (20.5% O_2 in N_2). The samples were measured with a heating rate of 5 K/min up to a temperature of 1000 °C in an aluminum oxide crucible.

Scanning electron microscope (SEM) images were taken on a JSM-6510LV QSEM with a LaB_6 or with a tungsten cathode at 5–20 kV. The EDX measurements were performed with a Bruker Xflash 410 silicon drift detector with a Si(Li) semiconductor detector.

Nuclear magnetic resonance spectroscopy (NMR) were measured on a Bruker Avance III-600 or a Bruker Avance III-300 NMR spectrometer at 298 K. ^{1}H NMR Spectra were referenced to the residual proton solvent signal in D_2O/NaOD, set at 4.79 ppm. Approximately 10 mg of each sample was dissolved under decomposition in 5% NaOD/D_2O. The subsequently filtered solution, using a syringe filter, was transferred into an NMR tube. NMR spectra are shown in Section S4 in the Supp. Info.

Elemental analyses were measured on an ELEMENTAR vario MICRO cube.

Synthesis of MIL-160

The synthesis of MIL-160(Al) was performed using the synthesis recently reported from Permyakova *et al*[55] In a typical reaction 2,5-furandicarboxylic acid ($C_4OH_2(COOH)_2$, 624 mg, 4.0 mmol) and basic aluminum diacetate ($Al(OH)(CH_3COO)_2$, 648 mg, 4.0 mmol) were dissolved in 4 mL of deionized Millipore water and refluxed (100 °C) for 24 h. Different amounts of modulator were added to the batches before refluxing in molar modulator:metal/linker ratios up to 2:1 (see Table S1, Supp. Info. for details). Formic acid, acetic acid, oxalic acid and hydrochloric acid were used as modulators. After 24 h the precipitated product was separated by centrifugation and washed three times each with water (3 × 35 mL) and ethanol (3 × 35 mL). Subsequently, the product was dried under air for 12 h at 80 °C. Yields are given in the Supp. Info. in Table S1.

Acknowledgements

Funding by the German Federal Ministry of Education and Research (BMFT) for the project Optimat under grant 03SF0492C is gratefully acknowledged. Open Access funding enabled and organized by Projekt DEAL.

Conflict of Interest

The authors declare no conflict of interest.

Data Availability Statement

The data that support the findings of this study are available from the corresponding author upon reasonable request.

Keywords: MOF-modulation · metal-organic-framework · MIL-160 · modulator · aluminum MOF

[1] S. R. Batten, N. R. Champness, X.-M. Chen, J. Garcia-Martinez, S. Kitagawa, L. Öhrström, M. O'Keeffe, M. Paik Suh, J. Reedijk, *Pure Appl. Chem.* **2013**, *85*, 1715–1724.
[2] H.-C. Zhou, J. R. Long, O. M. Yaghi, *Chem. Rev.* **2012**, *112*, 673–674.
[3] A. Kirchon, L. Feng, H. F. Drake, E. A. Joseph, H.-C. Zhou, *Chem. Soc. Rev.* **2018**, *47*, 8611–8638.
[4] C. Janiak, J. K. Vieth, *New J. Chem.* **2010**, *34*, 2366–2388.
[5] M. Taddei, *Coord. Chem. Rev.* **2017**, *343*, 1–24.
[6] X. Liu, X. Wang, F. Kapteijn, *Chem. Rev.* **2020**, *120*, 8303–8377.
[7] D. M. Steinert, S.-J. Ernst, S. K. Henninger, C. Janiak, *Eur. J. Inorg. Chem.* **2020**, *2020*, 4502–4515.
[8] F. Jeremias, D. Fröhlich, C. Janiak, S. Henninger, *New J. Chem.* **2014**, *38*, 1846–1852.
[9] S. M. J. Rogge, A. Bavykina, J. Hajek, H. Garcia, A. I. Olivos-Suarez, A. Sepúlveda-Escribano, A. Vimont, G. Clet, P. Bazin, F. Kapteijn, M. Daturi, E. V. Ramos-Fernandez, F. X. Llabrés i Xamena, V. Van Speybroeck, J. Gascon, *Chem. Soc. Rev.* **2017**, *46*, 3134–3184.

[10] K. Adil, Y. Belmabkhout, R. S. Pillai, A. Cadiau, P. M. Bhatt, A. H. Assen, G. Maurin, M. Eddaoudi, *Chem. Soc. Rev.* **2017**, *46*, 3402–3430.
[11] J. Dechnik, J. Gascon, C. J. Doonan, C. Janiak, C. J. Sumby, *Angew. Chem. Int. Ed.* **2017**, *56*, 9292–9310; *Angew. Chem.* **2017**, *129*, 9420–9439.
[12] J. A. Mason, M. Veenstra, J. R. Long, *Chem. Sci.* **2014**, *5*, 32–51.
[13] Y. He, W. Zhou, G. Qian, B. Chen, *Chem. Soc. Rev.* **2014**, *43*, 5657–5678.
[14] E. Alvarez, N. Guillou, C. Martineau, B. Bueken, B. Van de Voorde, C. Le Guillouzer, P. Fabry, F. Nouar, F. Taulelle, D. de Vos, J.-S. Chang, K. H. Cho, N. Ramsahye, T. Devic, M. Daturi, G. Maurin, C. Serre, *Angew. Chem. Int. Ed.* **2015**, *54*, 3664–3668; *Angew. Chem.* **2015**, *127*, 3735–3739.
[15] D. S. Sholl, R. P. Lively, *J. Phys. Chem. Lett.* **2015**, *6*, 3437–3444.
[16] Z. Fang, B. Bueken, D. de Vos, R. A. Fischer, *Angew. Chem. Int. Ed.* **2015**, *54*, 7234–7254; *Angew. Chem.* **2015**, *127*, 7340–7362.
[17] S. Dissegna, K. Epp, W. R. Heinz, G. Kieslich, R. Fischer, *Adv. Mater.* **2018**, *30*, 1704501.
[18] J. Ren, M. Ledwaba, N. M. Musyoka, H. W. Langmi, M. Mathe, S. Liao, W. Pang, *Coord. Chem. Rev.* **2017**, *349*, 169–197.
[19] G. Wißmann, A. Schaate, S. Lilienthal, I. Bremer, A.A. Schneider, P. Behrens, *Microporous Mesoporous Mater.* **2011**, *152*, 64–70.
[20] B. Moll, T. Müller, C. Schlüsener, A. Schmitz, P. Brandt, S. Öztürk, C. Janiak, *Mater. Adv.* **2021**, *2*, 804–812.
[21] M. Kalaj, K. C. Bentz, S. Ayala Jr, J. M. Palomba, K. S. Barcus, Y. Katayama, S. M. Cohen, *Chem. Rev.* **2020**, *120*, 16, 8267–8302.
[22] T. Tsuruoka, S. Furukawa, Y. Takashima, K. Yoshida, S. Isoda, S. Kitagawa, *Angew. Chem. Int. Ed.* **2009**, *48*, 4739–4743; *Angew. Chem.* **2009**, *121*, 4833–4837.
[23] A. Umemura, S. Diring, S. Furukawa, H. Uehara, T. Tsuruoka, S. Kitagawa, *J. Am. Chem. Soc.* **2011**, *133*, 15506–15513.
[24] S. Diring, S. Furukawa, Y. Takashima T Tsuruoka, S. Kitagawa, *Chem. Mater.* **2010**, *22*, 4531–4538.
[25] G. C. Shearer, S. Chavan, S. Bordiga, S. Svelle, U. Olsbye, K. P. Lillerud, *Chem. Mater.* **2016**, *28*, 3749–3761.
[26] S. Gökpinar, T. Diment, C. Janiak, *Dalton Trans.* **2017**, *46*, 9895–9900.
[27] I. A. Lazaro, C. J. R. Wells, R. S. Forgan, *Angew. Chem. Int. Ed.* **2020**, *59*, 5211–5217; *Angew. Chem.* **2020**, *132*, 5249–5255.
[28] Y. Liao, L. Zhang, M. H. Weston, W. Morris, J. T. Hupp, O. K. Farha, *Chem.Commun.* **2017**, *53*, 9376-3979.
[29] A. J. Rieth, A. M. Wright, M. Dincă, *Nat. Rev. Mater.* **2019**, *4*, 708–725.
[30] L. Helm, A. E. Merbach, *Coord. Chem. Rev.* **1999**, *187*, 151–181.
[31] L. Helm, G. M. Nicolle, A. E. Merbach, *Adv. Inorg. Chem.* **2005**, *57*, 327–379.
[32] S. E. Lincoln, *Helv. Chim. Acta* **2005**, *88*, 523–545.
[33] T. Zhao, F. Jeremias, I. Boldog, B. Nguyen, S. K. Henninger, C. Janiak, *Dalton Trans.* **2015**, *44*, 16791.
[34] T. Zhao, L. Yang, P. Feng, I. Gruber, C. Janiak, Y. Liu, *Inorg. Chim. Acta* **2018**, *471*, 440–445.
[35] T. Zhao, S. Li, Y.-X. Xiao, C. Janiak, G. Chang, G. Tian, X.-Y. Yang, *Sci. China Mater.* **2021**, *64*, 252–258.
[36] L. Yang, T. Zhao, I. Boldog, C. Janiak, X.-Y. Q. Li, Y.-J. Zhou, Y. Xia, D.-W. Lai, Y.-J. Liu, *Dalton Trans.* **2019**, *48*, 989–996.
[37] T. D. Bennett, A. K. Cheetham, A. H. Fuchs, F.-X. Coudert, *Nat. Chem.* **2016**, *9*, 11–16.
[38] H. W. B. Teo, A. Chakraborty, S. Kayal, *Microporous Mesoporous Mater.* **2018**, *272*, 109–116.
[39] T. Loiseau, C. Serre, C. Huguenard, G. Fink, F. Taulelle, M. Henry, T. Bataille, G. Férey, *Chem. Eur. J.* **2004**, *10*, 1373–1382.
[40] C. Kiener, U. Müller, M. Schubert, Germany Pat. WO2007/118841 A2, BASF SE, **2007**.
[41] C. Kiener, U. Müller, M. Schubert, US Pat. 12/297,666, BASF SE, **2012**.
[42] E. Leung, U. Müller, N. Trukhan, H. Mattenheimer, G. Cox, US Pat. 13/249,943, BASF SE, **2012**.
[43] H. Reinsch, M. A. van der Veen, B. Gil, B. Marszalek, T. Verbiest, D. de Vos, N. Stock, *Chem. Mater.* **2013**, *25*, 17–26.
[44] A. Cadiau, J. S. Lee, D. D. Borges, P. Fabry, T. Devic, M. T. Wharmby, C. Martineau, D. Foucher, F. Taulelle, C.-H. Jun, Y. K. Hwang, N. Stock, M. F. De Lange, F. Kapteijn, J. Gascon, G. Maurin, J.-S. Chang, C. Serre, *Adv. Mater.* **2015**, *27*, 4775–4780.
[45] M. Gaab, N. Trukhan, S. Maurer, R. Gummaraju, U. Müller, *Microporous Mesoporous Mater.* **2012**, *157*, 131–136.
[46] F. Jeremias, D. Fröhlich, C. Janiak, S. K. Henninger, *RSC Adv.* **2014**, *4*, 24073–24082.
[47] D. Fröhlich, S. K. Henninger, C. Janiak, *Dalton Trans.* **2014**, *43*, 15300–15304.
[48] D. Fröhlich, E. Pantatosaki, P. D. Kolokathis, K. Markey, H. Reinsch, M. Baumgartner, M. A. van der Veen, D. E. de Vos, N. Stock, G. K. Papadopoulos, S. K. Henninger, C. Janiak, *J. Mater. Chem. A* **2016**, *4*, 11859–11869.
[49] P. Brandt, S.-H. Xing, J. Liang, G. Kurt, A. Nuhnen, O. Weingart, C. Janiak, *ACS Appl. Mater. Interfaces* **2021**, *13*, 29137–29149.
[50] F. Jeremias, A. Khutia, S. K. Henninger, C. Janiak, *J. Mater. Chem.* **2012**, *22*, 10148–10151.
[51] A. Samokhvalov, *Coord. Chem. Rev.* **2018**, *374*, 236–253.
[52] P. Brandt, A. Nuhnen, M. Lange, J. Möllmer, O. Weingart, C. Janiak, *ACS Appl. Mater. Interfaces* **2019**, *11*, 17350–17358.
[53] http://avantium.com/yxy/yxy-technology.html; accessed 01.08.**2017**, 01:54 h.
[54] Press releases: 'Synvina: Jointventure of BASF and Avantium established', **2016**.
[55] A. Permyakova, O. Skrylnyk, E. Courbon, M. Affram, S. Wang, U.-H. Lee, A. H. Valekar, F. Nouar, G. Mouchaham, T. Devic, G. De Weireld, J.-S. Chang, N. Steunou, M. Frère, C. Serre, *ChemSusChem.* **2017**, *10*, 1419–1426.
[56] S. Canossa, A. Gonzalez-Nelson, L. Shupletsov, M. del Carmen Martin, M. A. van der Veen, *Chem. Eur. J.* **2020**, *26*, 3564–3570.
[57] H. W. B. Teo, A. Chakraborty, S. Kayal, *Microporous Mesoporous Mater.* **2018**, *272*, 109–116.
[58] M. Wahiduzzaman, D. Lenzen, G. Maurin, N. Stock, M. T. Wharmby, *Eur. J. Inorg. Chem.* **2018**, *2018*, 3626–3632.
[59] E. Martuscelli, C. Pedone, *Acta Crystallogr. Sect. B* **1968**, *24*, 175.
[60] G. C. Shearer, S. Chavan, J. Ethiraj, J. G. Vitillo, S. Svelle, U. Olsbye, C. Lamberti, S. Bordiga, K. P. Lillerud, *Chem. Mater.* **2014**, *26*, 4068–4071.
[61] H. Hopff, A. Krieger, *Helv. Chim. Acta* **1961**, *44*: 1058–1063.
[62] M. Tommes, K. Kaneko, A. V. Neimark, J. P. Olivier, F. Rodriguez-Reinoso, J. Rouquerol, K. S. W. Sing, *Pure Appl. Chem.* **2015**, *87*, 1051–1069.

Manuscript received: December 11, 2021
Revised manuscript received: January 17, 2022
Accepted manuscript online: January 25, 2022

